Localizing Atrial Flutter Circuit using Variability in the Vectorcardiographic Loop Parameters

Muhammad Haziq Kamarul Azman[1 2], Olivier Meste[1], Kushsairy Kadir[2], Decebal Gabriel Latcu[3]

[1] Université Côte d'Azur, CNRS, I3S, France
[2] Universiti Kuala Lumpur, Malaysia
[3] Cardiology Department, Centre Hospitalier Princesse Grace, Monaco

Abstract

Atrial flutter circuit localization is usually determined during a catheter ablation procedure. Knowledge of this information beforehand could aid clinicians assess and plan the operation in advance to improve efficacy. Variability as a marker to discriminate localization non-invasively was suggested in the literature, and evaluated by one group. However, variability may originate from respiratory motion which may affect right and left AFL differently. This is hypothesized to be the reason for difference in right and left AFL variability. To address this, we analyzed the effect of removing respiratory motion influence from f wave observations on classification accuracy. ECG records from patients with AFL were processed using a novel approach: respiratory motion was estimated and removed in order to recover variability intrinsic to AFL. Vectorcardiographic loop parameters were estimated from each observation and statistical measures of the set of parameter values were calculated before being fed into a classification algorithm. The results show that f waves are negligibly affected by respiratory motion. It is also possible to discriminate circuit localization with good accuracy.

1. Introduction

Knowledge of the characteristics of macro-reentrant tachyarrhythmia is crucial for a successful and quality catheter ablation: an increasingly popular treatment today, targeted towards atrial fibrillation and atrial flutter (AF and AFL). This information, however, is accessible only during the procedure itself. In the case of AFL, one significant information is the localization of the circuit: either the left or right atrium. The ability to estimate circuit localization prior to the procedure could aid clinicians in pre-operative assessment and planning in order to improve procedural efficacy.

The most common form of AFL is called typical AFL, associated with several stereotypic characteristics (right atrial localization and passage by a set of stable, well-defined obstacles). Atypical AFL is defined as any circuit that do not match one or either of the criteria. Both forms are observable via the electrocardiogram (ECG), allowing for a non-invasive analysis and estimation of the characteristics. As a result, information regarding the pathology can be made available without additional invasive operations. It was found that spatiotemporal coherence can predict a left localization with 84% sensitivity and 75% specificity [1]. Many other studies suggest its association with lower atrial activity regularity, and hence larger variability.

On the other hand, respiratory motion affects the ECG signal by shifting the electrical axis of the cardiac dipole. This is introduces artificial variability and it may be a reason why discrimination between right and left AFL was possible: consider the different location of the right and left atrium in the thoracic cavity. Right AFL may be affected differently than left AFL. If this variability is the origin of the difference between right and left AFL variability, then if removed, we expect right and left AFL to present similar variability, and hence cannot be discriminated. If it is not the origin of the difference, then removing its contribution may affect right and left AFL variability, but discrimination could still be done reliably. We aim to test this hypothesis by employing several novel approaches.

2. Methodology

The overall methodology is summarized by (Fig 1). All data processing and classification was done in MATLAB R2014b (MathWorks, USA).

2.1. Signal pre-processing

75 recordings of 12-leads ECG from the Centre Hospitalier Princesse Grace in Monaco were acquired from 68 patients reported with AFL during ablation procedures using an acquisition system (Bard, USA). All signals were sampled at 2000 Hz and are about 1 minute in length.

 ISSN: 2325-887X DOI: 10.22489/CinC.2018.355

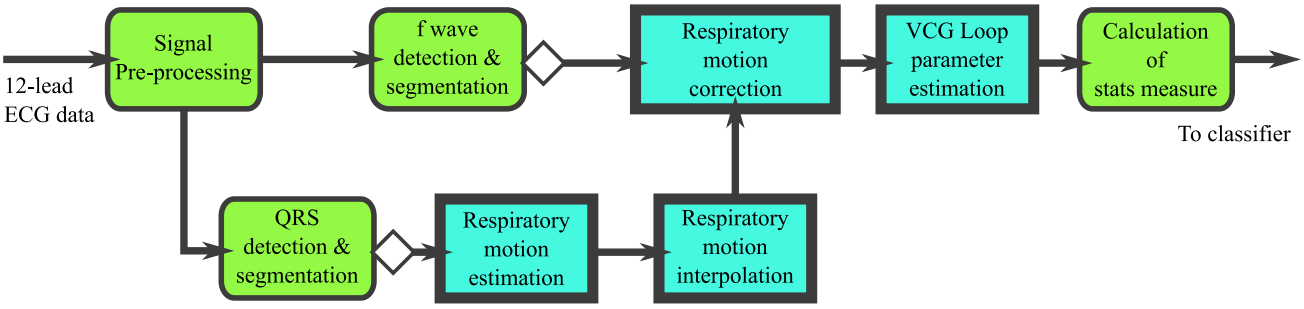

Figure 1. The methodology employed in this research. 12-lead ECG data is processed and undergoes a series of wave detection and segmentation followed by estimation of respiratory motion at the time instants of QRS. The motion is estimated between two consecutive QRS instants before it is used in the correction stage. VCG loop parameters are then estimated, and statistical measures calculated and fed to the classifier. The diamond at the edge of the boxes indicates an inverse Dower transform. Blue, bolded rectangular boxes correspond to novel approaches we employed in this research.

All signals were filtered between 0.5 and 70 Hz with type II Chebyshev low-pass and high-pass filters in order to reject physiological motion and high-frequency noises, whilst preserving f-wave onsets. A 50 Hz finite-impulse response notch filter was used to remove powerline noise.

Records that were unusable (missing leads, too noisy, atrio-ventricular block ratio <2:1) were excluded. Several records with 2:1 block ratio were kept, provided that several f wave beat was available. The total number of records at the end was 54, of which 24 were right AFL and 30 left AFL.

2.2. f wave detection and segmentation

The analysis targets f wave observations, present in the recording as a continuous, periodic atrial activity, partially overlapped by ventricular activity. Due to the high synchronicity between them, standard techniques to extract atrial activity (filtering, beat averaging, source separation) is bound to fail. We resort to working with segments of the atrial activity where the deflections are significant. We extracted these segments using a likelihood ratio-based detector described in [2].

2.3. Estimation and correction of respiratory motion

The estimation of respiratory motion from the ECG is a well-known topic of research. This is useful for e.g. cancelling unwanted influences caused by the periodic changes induced by respiration. An estimator based on least squares principle has been detailed and applied to the QRS realignment problem in vectorcardiograms (VCG) [3]. In a VCG representation comprised of three leads X, Y and Z, QRS complexes form a 3-dimensional loop.

We consider the dual formulation, suitable for operating on multiple loops:

$$\hat{\beta}_i, \hat{\mathbf{R}}_i = \arg\min_{\beta,\mathbf{R}} \|\beta \mathbf{X}_i \mathbf{R} - \mathbf{X}_R\|_F^2 \quad (1)$$

$$\hat{\mathbf{R}}_i = \mathbf{V}\mathbf{U}^{\mathrm{T}} \quad (2)$$

$$\mathbf{X}_R^{\mathrm{T}}\mathbf{X}_i = \mathbf{U}\mathbf{\Sigma}\mathbf{V}^{\mathrm{T}}$$

$$\hat{\beta}_i = \frac{\mathrm{tr}(\mathbf{X}_{\mathrm{i}}\mathbf{X}_{\mathrm{i}}^{\mathrm{T}})}{\mathrm{tr}(\mathbf{X}_{\mathrm{i}}\hat{\mathbf{R}}_{\mathrm{i}}\mathbf{X}_{\mathrm{R}}^{\mathrm{T}})} \quad (3)$$

where β represents loop scaling and $\mathbf{R}$ loop rotation ($\mathbf{X} \in \mathbb{R}^{N\times 3}$). Three rotation angles ϕ_X, ϕ_Y, ϕ_Z: one for each axis, can be obtained from the matrix $\mathbf{R}$, available at every QRS time instant. The i-th QRS loop $\mathbf{X}_i$ is assumed properly aligned with the reference $\mathbf{X}_R$; we omit a third effect (temporal alignment) considered in his article.

The high signal-to-noise ratio of QRS complexes allow a reliable estimate of respiratory motion at each QRS instant. On the other hand, respiratory motion is remarkably slow and has a low-frequency profile compared to cardiac frequency, which is several orders of magnitude higher. The estimates at each QRS instants should be sufficient to perform a reliable interpolation of parameter values to any time instant. These assumptions were used to obtain respiratory motion estimates at the time instant of f waves.

QRS complexes were segmented, transformed into VCG loops using the inverse Dower transform [4] and temporally resynchronized. A multipass algorithm was applied [3]. However, we observed that several rotation angles had values that are considered physiologically impossible (e.g. $\approx 80°$). These were caused by the estimator producing a matrix $\mathbf{R}_r$ which performs a reflection instead of rotation in order to minimize the least squares error [5]. To restrict the estimator to produce a strict rotation, we modified the estimation procedure.

Firstly, we modified the singular value decomposition (SVD) algorithm used to estimate $\mathbf{R}$. The singular vector $\mathbf{V}$ can be estimated using alternated least squares. In order

to maintain similar subspace direction, the algorithm was given as an initial point the singular vectors $\mathbf{V}_R$ derived from the reference loop ($\mathbf{X}_R^{\mathrm{T}}\mathbf{X}_R = \mathbf{U}_R\mathbf{\Sigma}_R\mathbf{V}_R^{\mathrm{T}}$). This ensures that the subspaces of the QRS loops are always aligned and do not present sign ambiguities: a problem well-known with SVD.

Next, the rotation matrix is tested for reflection by observing the value of $\det(\mathbf{U})\det(\mathbf{V})$, as was suggested in [5]. A value of -1 indicates a reflection, and the corresponding correction is made by calculating $\tilde{\mathbf{R}} = \mathbf{V}\mathbf{S}\mathbf{U}^{\mathrm{T}}$ where

$$\mathbf{S} = \begin{cases} \mathbf{I}, & \text{if } \det(\mathbf{U})\det(\mathbf{V}) = 1 \\ \mathrm{diag}(1,1,-1), & \text{if } \det(\mathbf{U})\det(\mathbf{V}) = -1 \end{cases} \quad (4)$$

The alignment algorithm was applied only for a single pass. Respiratory motion parameters, given by β and $(\phi_X\ \phi_Y\ \phi_Z)$ were then interpolated using piecewise cubic Hermite interpolants to avoid unstable, non-monotonic estimate between two knots. Scale and angle values were then taken at the time instant of each f waves (also transformed into VCG) and were used to obtain the corrected individual loop $\tilde{\mathbf{F}}_i$:

$$\tilde{\mathbf{F}}_i = \tilde{\beta}_i \mathbf{F}_i \tilde{\mathbf{R}}_i \quad (5)$$

$$\tilde{\mathbf{R}} = \begin{bmatrix} 1 & 0 & 0 \\ 0 & \cos\phi_X & \sin\phi_X \\ 0 & -\sin\phi_X & \cos\phi_X \end{bmatrix} * \begin{bmatrix} \cos\phi_Y & 0 & \sin\phi_Y \\ 0 & 1 & 0 \\ -\sin\phi_Y & 0 & \cos\phi_Y \end{bmatrix} * \begin{bmatrix} \cos\phi_Z & \sin\phi_Z & 0 \\ -\sin\phi_Z & \cos\phi_Z & 0 \\ 0 & 0 & 1 \end{bmatrix}$$

with $\tilde{\beta}_i$ and $\tilde{\mathbf{R}}_i$ the value of the interpolated motion at the time instant of the i-th f loop observation $\mathbf{F}_i$.

2.4. Estimation of loop parameters and statistical measures

VCG loop subspace parameters can be used to characterize AFL in the 3-dimensional space [6, 7]. The eigenvectors $\mathbf{V} = [\mathbf{v}_1\ \mathbf{v}_2\ \mathbf{v}_3]$ and singular values $[\lambda_1\ \lambda_2\ \lambda_3]$ issued from the singular value decomposition of the loops were used to calculate these parameters for each f loop observation. The 4 parameters employed here were the same as ones in our previous paper [8].

The first two parameters (ϕ_{AZ}, ϕ_{EL}) capture the VCG loop subspace direction and the remaining two parameters (ψ_{PL}, ψ_{PG}) describe the form of the loop in 3-dimensional space (i.e. whether it is flat or occupies space, and circular or elliptic). These 4 parameters vary from beat to beat.

Post-processing was applied before calculating the parameters (truncation to remove edge effects of T wave correction, downsampling to 250 Hz, point redistribution using spline interpolation to ensure equidistance in the 3-dimensional space).

The parameters ϕ_{AZ} and ϕ_{EL} are prone to an ambiguity of $\pm 180°$, inherited from the sign ambiguity of eigenvectors. This introduces artificial variability in the data. To correct this, we used a combinatory optimization method consisting of choosing each value as either ϕ or $\phi \pm 180°$ in order to minimize the variance of the set.

It could be suggested that typical and atypical AFL subspace direction may be different (i.e. $\phi_R \neq \phi_L$) [6]. Furthermore, AF organization has been quantified by the varying standard deviation of the 4 parameter values for different levels of organization [7]. In this light, we calculated several statistical measures on each of the series of 4 parameters. These measures quantify to an extent the variability contained in the set of f waves. The considered measures were the mean, standard deviation, variance, skewness and kurtosis. Each record is thus described by $4 \times 5 = 20$ features.

2.5. Classification scheme

The output of the processing chain was fed into a linear kernel support vector machine (SVM) with soft margin constraint and linear discriminant analysis (LDA) classifiers. Additionally, we are interested in finding the features that consistently produce a good classifier accuracy. To this end, we devised an iterative classification scheme which tests all possible combinations of features. The total number of combinations considered in this paper was $2^{20} - 1$ for combinations up to 20 features. (Fig 2) shows the maximum accuracy for each size of combination from 1 to 20 for the SVM classifier. The results of the LDA classifier show the same trend.

3. Results and Discussion

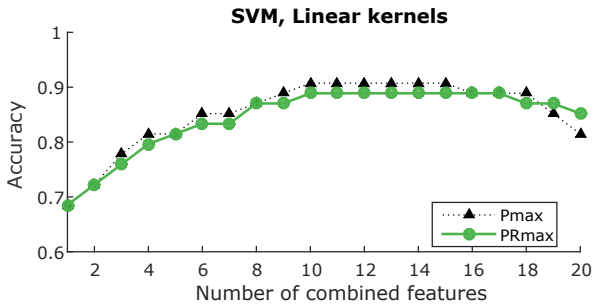

Figure 2. Classifier performance, given as the maximum accuracy for a given number of feature combination. The suffix 'R' indicate that respiratory motion was removed from the set of f waves. General accuracy increase is observed up to a combination of 10 features.

3.1. Effect of respiratory motion correction on AFL

Effect of respiratory motion on AFL was evaluated by processing f wave VCG loops to remove artificial variability respiratory motion. A set of f wave observations exhibiting only variability intrinsic to AFL was obtained at the end. We analyzed the change in variability by performing a Bland-Altman analysis on the standard deviation of each of the 4 loop parameters before and after correction. Variability before correction should indeed be greater than after correction.

For parameter ϕ_{AZ}, the difference was -0.242 ± 2.375 and for ϕ_{EL}, it was -0.500 ± 5.424, given as the median $\pm$ the mean absolute deviation ($p < 0.05$). We observe a larger variability than before correction was applied, shown by the negative values. This suggests that correcting f waves added artificial variability into the observation. However, referring to (Fig 2), we see that the classifier performance using the corrected loops was not greatly affected. Thus overall, these results suggest that respiratory motion introduces variability in f wave loops, but does not explain the overall variability observed, and that right and left AFL may be intrinsically different.

The parameter ψ was not affected as a scale and rotation operation do not modify the loop morphology.

3.2. Comparison of classification accuracy

An example of the classifier result is shown in (Fig 2). Good classification accuracy is achieved using features obtained from the set of 4 loop parameters ϕ_{AZ}, ϕ_{EL}, ψ_{PL} and ψ_{PG}. The maximum accuracy obtained was 0.91 when considering a minimum of 10 features, corresponding to a sensitivity and specificity of 90% and 92%. Accuracy increases as the number of combined features increase but drops after a minimum combination of 15 features. This suggests that right and left AFL are different with regards to a combination of several features, but above a certain length of combination, they are essentially similar. To remedy this problem, more patients need to be used.

Best features were determined by observing the number of times a feature was used in a combination that produces the maximum accuracy, for all length of combinations from 1 to 20. We found that the skewness of parameter ψ_{PL} and the mean of parameter ψ_{PG} occur frequently in many of these combinations. Although this leads to believe that these features should be used to construct a practical classifier, they are not the only features that constitute the best combination: several others also provide useful information in discriminating right and left AFL. Rather, it can be said that right and left AFL are different in regards to these features. Further analysis is needed to better understand how right and left AFL may be different.

4. Conclusion

We present in this paper several items and conclusions. First, we tested the hypothesis that variability in AFL was due to the variability introduced by respiratory motion which might affect right and left AFL differently. Using a novel approach, we concluded that f waves were minimally affected by respiratory motion and that the variability observed in the ECG was intrinsic to AFL. By exploiting this variability, good discrimination between right and left atrial flutter localization was achieved.

Acknowledgements

This work was realized with the support from Universiti Kuala Lumpur and the French government.

References

[1] Kahn AM, Krummen DE, Feld GK, Narayan SM. Localizing circuits of atrial macro-reentry using ECG planes of coherent atrial activation. Hear Rhythm 2007;4(4):445–451.

[2] Kamarul Azman MH, Meste O, Kadir K. Detecting flutter waves in the electrocardiogram using generalized likelihood ratio test. In Computing in Cardiology, volume 45. September 2018; .

[3] Sornmo L. Vectorcardiographic loop alignment and morphologic beat-to-beat variability. IEEE Transactions on Biomedical Engineering December 1998;45(12):1401–1413.

[4] Dower GE, Machado HB, Osborne JA. On deriving the electrocardiogram from vectoradiographic leads. Clin Cardiol apr 1980;3(2):87–95.

[5] Umeyama S. Least-squares estimation of transformation parameters between two point patterns. IEEE Transactions on pattern analysis and machine intelligence 1991;13(4):376–380.

[6] Ng J, Sahakian AV, Fisher WG, Swiryn S. Atrial flutter vector loops derived from the surface ECG: does the plane of the loop correspond anatomically to the macroreentrant circuit? J Electrocardiol 2003;36:181–186.

[7] Richter U, Stridh M, Bollmann A, Husser D, Sörnmo L. Spatial characteristics of atrial fibrillation electrocardiograms. J Electrocardiol 2008;41:165–172.

[8] Kamarul Azman MH, Meste O, Kadir K, Latcu DG. Estimation and removal of T wave component in atrial flutter ecg to aid non-invasive localization of ectopic source. In Computing in Cardiology, volume 44. September 2017; 376–380.

Address for correspondence:

Muhammad Haziq Kamarul Azman
Bureau 206
Laboratoire I3S
2000 route des Lucioles
06900 Sophia Antipolis, France
mhaziq@unikl.edu.my